DOI: 10.24996/ijs.2026.67.5.38

ISSN: 0067-2904

A Novel Robust Approach of Optimized Hybrid Watermarking Scheme for Color Images Using DWT, DCT, Permutation, and PSO

Luqman Mohammed Mustafa[1]*, Dr. Harith Raad Hasan[2]

[1]*Technical College of Informatics, Sulaimani Polytechnic University, Sulaimani, Kurdistan Region, Iraq.*

[1]*Computer Science, College of Basic Education, University of Sulaimani, KRG, Iraq*

[2]*Department of Software Engineering, Faculty of Engineering and Computer Science, Qaiwan International University (QIU), Sulaymaniyah, Iraq.*

Received: 20/2/2025 Accepted: 1/6/2025 Published: xx

Abstract

This paper presents a novel digital image watermarking technique for color images that integrates discrete wavelet transforms (DWT), discrete cosine transforms (DCT), permutation scrambling, and particle swarm optimization algorithms (PSO). In the trade-offs of resilience and imperceptibility, it is a method that will be extended to improve both for efficient watermarking. To improve the security, we first randomize the watermark image using a permutation and then perform DCT on it to obtain its coefficients. The coefficients are embedded through the optimal scaling factor estimated by the PSO into the DWT sub-bands of the host color image. This optimization provides a trade-off with a reasonable amount between the fidelity and robustness of the watermarked image. The proposed approach surpasses 49 dB in peak signal-to-noise ratio (PSNR), hence indicating superior imperceptibility of the watermark. Moreover, it has significant resilience against several conventional image processing methods, with normalized correlation coefficients (NCC) consistently around 1.0. An optimizing approach using PSO ensures little visual distortion and maintains robustness, overcoming limitations observed in alternative approaches. Experimental results validate the technique's efficacy in improving both the invisibility and strength of digital image watermarking.

Keywords: discrete wavelet transform, discrete cosine transform, permutation, PSO, optimization, Hybrid

نهج قوي ومبتكر لنظام وسم مائي هجين ومحسّن للصور الملونة باستخدام تحويل المويجات المتقطع *(DWT)*، وتحويل جيب التمام المتقطع *(DCT)* ، والتبديل، وخوارزمية تحسين سرب الجسيمات *(PSO)*

لوقمان محمد مصطفى[1]، د.حارث رعد حسن[2]

[1]الكلية التقنية للمعلوماتية، جامعة السليمانية التقنية، السليمانية، العراق.

[1]علوم الحاسوب، كلية التربية الأساسية، جامعة السليمانية، إقليم كردستان، العراق.

[2]قسم هندسة البرمجيات، كلية الهندسة وعلوم الحاسوب، جامعة قيوان الدولية، السليمانية، العراق.

*Email: Luqman.mohammed.tci@spu.edu.iq

الملخص

يقدّم هذا البحث تقنية جديدة لإخفاء العلامات المائية في الصور الرقمية الملوّنة، من خلال دمج التحويل المويجي المتقطع (DWT) والتحويل الجيبي المتقطع (DCT) وتقنية تشويش الترتيب (Permutation Scrambling)وخوارزمية تحسين أسراب الجسيمات .(PSO) تهدف الطريقة المقترحة إلى تحقيق توازن فعّال بين المتانة وعدم الوضوح، وهما من العوامل الحاسمة في تقنيات العلامات المائية. ولتعزيز الأمان، يتم أولًا تشويش صورة العلامة المائية باستخدام ترتيب عشوائي، ثم يُطبَّق عليها تحويل DCT لاستخراج معاملات التردد. تُضمَّن هذه المعاملات في نطاقات DWT للصورة الأصلية باستخدام معامل تحجيم مثالي يتم تحديده من خلال خوارزمية .PSO يسهم هذا التحسين في تحقيق توازن مناسب بين جودة الصورة ومتانة العلامة المائية. أظهرت النتائج التجريبية أن الطريقة المقترحة تحقق نسبة إشارة إلى ضوضاء ذروية (PSNR) تتجاوز 49 ديسيبل، مما يدل على مستوى عالٍ من عدم الوضوح (الخفاء). بالإضافة إلى ذلك، أثبتت الطريقة قدرة كبيرة على مقاومة الهجمات التقليدية في معالجة الصور، حيث بلغت معاملات الارتباط المُطَبَّعة (NCC) قيمًا قريبة من 1.0 بشكل مستمر. من خلال استخدام PSO في عملية التحسين، تضمن التقنية تشويشًا بصريًا ضئيلًا مع الحفاظ على قوة العلامة المائية، مما يتجاوز القيود الموجودة في الأساليب البديلة. تؤكد النتائج فعالية الطريقة المقترحة في تحسين كل من خفاء العلامة المائية ومتانتها في الصور الرقمية.

1. Introduction

In the contemporary digital age, digital watermarking is considered a basic need for intellectual property rights protection and authenticity of digital media [1]. The proliferation of online multimedia distribution has led to a high demand for ownership protection and prevention of unauthorized alteration of digital photographs [2]. The backbone of an efficient watermarking system must fulfil two basic requirements: The first one is imperceptibility, where the message hides in a manner that the watermark does not reduce the visual quality of the host image and second is the robustness which should ensure that the watermark remains intact under several processing operations like compression, filtering or geometric transformations.

Strategies that enhance hybrid watermarking have gained prominence in recent years due to the effective algorithms that include many transformations and techniques. Combining discrete wavelet transforms and discrete cosine transforms has proven highly beneficial. DWT enables a multi-resolution perspective on the host picture, enabling precise embedding into sub-bands that enhance both imperceptibility and robustness. This paper [3] compares three transform domain techniques for digital image watermarking: Discrete Cosine Transformation, Discrete Wavelet Transformation, and Singular Value Decomposition. It finds that DWT outperforms DCT and SVD in robustness against various attacks, highlighting its effectiveness in watermarking applications. Yadav [4] analyzes image watermarking techniques utilizing particle swarm optimization with DCT and DWT. It indicates that integrating both improves watermark embedding and resistance to attacks. Another hybrid approach [5] employs Integer Wavelet Transform and Singular Value Decomposition to enhance the resilience and security of watermarks. It employs a genetic approach for optimizing quantization step size and strengthens the decryption process using encryption and a dual-component architecture. Yasmeen et al. [6] also introduced a hybrid watermarking technique that integrates Discrete Wavelet Transform and Singular Value Decomposition for the imperceptible embedding of watermarks in digital images. This approach enhances image security and increases resistance to degradation. The watermark is integrated into both grayscale and color images through the modification of the wavelet, particularly utilizing the HH component of the host image. The multi-level DWT transformation effectively captures essential features of the host image, whereas SVD extracts singular values that are integrated into the image.

Iwut et al. [7] introduce an approach for image watermarking utilizing the Discrete Cosine Transform (DCT) and the Genetic Algorithm. The approach enhances characteristics such as block size and color space, augmenting watermark resilience against attacks like JPEG compression and additive noise. In another research, Takore et al. [8] present a watermarking method that improves the resilience and imperceptibility of digital photographs. It employs the Lifting Wavelet Transform (LWT) hybrid transformation technique to mitigate challenges such as intensity calculation and rounding inaccuracies. Particle Swarm Optimization is employed to enhance the scaling factor. A new image watermarking approach by Laxmanika et al. [9] uses advanced methods such as discrete wavelet transform, bi-dimensional empirical mode decomposition, and particle swarm optimization, ensuring superior watermarked images while enhancing security and perceptual quality.

This paper proposes a new hybrid watermarking technique aimed at imperceptible and robust image watermarking, using DWT, permutation, DCT, and PSO. The approach uses DWT level three to decompose the RGB cover image into several distinct sub-bands. Then, a watermark image is converted to a permutation space aided by permutation indices and then modified by DCT. The LH3 of each color channel of the cover image is used for embedding the DCT-permuted watermark image. Moreover, the PSO optimizes the scaling factor for the sub-band container to ensure a balance between imperceptibility and robustness. Furthermore, PSO is used to optimize the scaling factor for the sub-band container to ensure a balance between imperceptibility and robustness, due to its efficiency in handling non-linear and high-dimensional optimization problems (detailed in Section 6). The method demonstrates resilience against attacks and remains imperceptible, proving effective for copyright protection and image transmission in multimedia contexts.

2. Preliminaries

2.1. Discrete Wavelet Transform (DWT)

The discrete wavelet transform is a frequency domain technique, and it is widely used in image processing [10]. And DWT outperforms other methods in generating robust and imperceptible results for watermarking. This method offers a comprehensive analysis of the alterations in an image, particularly in image watermarking [11], owing to its effective spatiotemporal localization and compatibility with the human visual system [12].

DWT decomposes an image into four sub-bands: one low-frequency band (LL) and three high-frequency bands (LH, HL, HH) [13]. Additional decomposition can be achieved by recursively partitioning the LL sub-band, which preserves the majority of the picture energy and low-frequency data. The LL sub-band is crucial for maintaining picture quality, but watermarking often occurs in one of the other three sub-bands associated with higher frequency components [10][14].

We employ a three-level Daubechies wavelet (DB2) to decompose the original image into sub-images, leading to LL, LH, HL, and HH components at the first level. The second and third levels further break down the LL sub-band, capturing higher frequency components. DB2 is chosen for its balance between computational efficiency and its ability to capture smooth variations in image data, which is advantageous for robust watermark embedding. The DB2 wavelet employs suitable scaling and wavelet filter coefficients for low-pass filtering, as shown in Eq. (1), and high-pass filtering, as specified in Eq. (2), applied to the image's rows and columns, subsequently down-sampling to produce the four sub-bands as illustrated in Fig. 1.

<table>
<tr><td>LL3</td><td>LH3</td><td rowspan="2">LH2</td><td rowspan="3">LH1</td></tr>
<tr><td>HL3</td><td>HH3</td></tr>
<tr><td colspan="2">HL2</td><td>HH2</td></tr>
<tr><td colspan="3">HL1</td><td>HH1</td></tr>
</table>

Figure 1: Three-level DWT on the LL sub-band

3. Mathematical Model

Utilizing a three-level Daubechies wavelet (DB2), we decompose the original image into sub-images, resulting in first-level LL, LH, HL, and HH components. The second and third layers decompose the LL sub-band by capturing higher frequency components. The DB2 wavelet, when applied to the image's rows and columns, employs appropriate scaling and wavelet filter coefficients for low-pass filtering, as shown in Eq. (1), and high-pass filtering, as outlined in Eq. (2), followed by down-sampling to produce the four sub-bands seen in Fig. 1.

3.1 DB2 decomposition equations

For each level of decomposition:

3.1.1 Low-pass filtering (scaling function):

$$\mathbf{L[n]} = \sum_{\mathbf{k}} \mathbf{x[k]}.\mathbf{h[n-2k]} \quad (1)$$

Where:

- $x[k]$: Input signal (e.g., rows or columns of the image).
- $h[n]$: Is the low pass filter coefficient (scaling filter).
- n: Is the output index of down-sampling.

3.1.2 High-pass filtering (wavelet function):

$$\mathbf{H[n]} = \sum_{\mathbf{k}} \mathbf{x[k]}.\mathbf{g[n-2k]} \quad (2)$$

Where:

- $g[n]$: High-pass filter coefficients (wavelet filter).

3.2 Filter Coefficients for DB2

The following coefficient filters are used by the Daubechies wavelet of type 2 (DB2):

3.2.1 Low-pass filter coefficients (scaling function):

$$\mathbf{h[n]} = \left[\frac{\mathbf{1+\sqrt{3}}}{\mathbf{4\sqrt{2}}}, \frac{\mathbf{3+\sqrt{3}}}{\mathbf{4\sqrt{2}}}, \frac{\mathbf{3-\sqrt{3}}}{\mathbf{4\sqrt{2}}}, \frac{\mathbf{1-\sqrt{3}}}{\mathbf{4\sqrt{2}}}\right] \quad (3)$$

3.2.2 High-pass filter coefficients (wavelet function):

$$\mathbf{g[n]} = \left[-\frac{\mathbf{1-\sqrt{3}}}{\mathbf{4\sqrt{2}}}, \frac{\mathbf{3-\sqrt{3}}}{\mathbf{4\sqrt{2}}}, \frac{\mathbf{3+\sqrt{3}}}{\mathbf{4\sqrt{2}}}, \frac{\mathbf{1+\sqrt{3}}}{\mathbf{4\sqrt{2}}}\right] \quad (4)$$

The filter coefficients will be applied iteratively at each level of breakdown, ultimately separating distinct frequency components within the image.

4. Discrete Cosine Transform (DCT)

The Discrete Cosine Transform (DCT) is an orthogonal transformation utilized in image and signal processing. DCT exhibits significant computational complexity, a low error rate, and a high compression ratio [10]. It converts the image from its spatial domain to a standardized frequency domain [8], representing the image as the summation of cosine functions with varying frequencies [12] [15]. The DCT rendering is appropriate for applications like JPEG

compression [2]. It converts empirical data into a genuine spectrum and minimizes redundancy by highlighting the essential frequency components [10].

In watermarking, the image is partitioned into different blocks, and each block is converted to a frequency domain with the Discrete Cosine Transform. High frequencies indicate complex details, whereas low frequencies include the complete visual structure. Watermarks are generally embedded by altering mid-frequency or high-frequency DCT coefficients to minimize the distortion. Furthermore, DCT II is the predominant kind, serving a fundamental function in JPEG compression.

The 2D-DCT for an image of dimensions $\boldsymbol{X} \times \boldsymbol{Y}$ is traditionally represented by a mathematical equation, as shown in Eq. (5), for an image.

$$\mathbf{X(u,v)} = \boldsymbol{\alpha}\mathbf{(u)}\boldsymbol{\alpha}\mathbf{(v)} \sum_{\mathbf{x=0}}^{\mathbf{X-1}} \sum_{\mathbf{y=0}}^{\mathbf{Y-1}} \mathbf{f(x,y)} \mathbf{cos}\left[\frac{\boldsymbol{\pi}\mathbf{(2x+1)u}}{\mathbf{2X}}\right] \mathbf{cos}\left[\frac{\boldsymbol{\pi}\mathbf{(2y+1)v}}{\mathbf{2Y}}\right] \quad (5)$$

Where:

- $X(u,v)$: DCT coefficients inside the frequency domain.
- $f(x,y)$: pixel values inside the spatial domain.
- u,v: frequency indices in the horizontal and vertical directions, respectively.
- $\alpha(u)\ and\ \alpha(v)$: normalization coefficients.

This equation calculates the 2D-DCT of the image by converting the spatial domain representation $f(x,y)$ into the frequency domain $X(u,v)$, including both horizontal and vertical frequency components.

5. Permutation Scrambling

A permutation is a reorganization of the components of an ordered collection or sequence. In image processing and watermarking, it is employed to obfuscate pixel values, coefficients, or image segments systematically to augment security and resilience. A permutation is defined as a bijective mapping of items, in which each element occurs precisely once in the rearranged set. In the watermarking field, permutation over elements (pixel locations, discrete cosine transform coefficients, and image blocks of size, e.g., 8x8 or 16x16) are schemes to increase the difficulty for an adversary to extract and/or insert watermarks. In this work, we employ a random shuffling method, where the pixel indices of the watermark are permuted using a pseudorandom sequence of indices generated with a fixed seed. This ensures both security and reproducibility, as the same seed can be used to reverse the permutation during extraction. This process is illustrated in Fig. 2, which demonstrates how permutation, which is the process of reordering items following a particular order of indices, and unpermutation, the inverse of permutation, reorders items back to their original positions. This method improves the watermark's security and resilience against attacks such as cropping and compression.

(a) (b)

Figure 2: (a) Watermark image (b) Watermark image after permutation

6. Particle Swarm Optimization for Scaling Factor

The scaling factor is a crucial parameter in image watermarking that profoundly influences both the watermark's resilience to attacks and the imperceptibility of the watermarked image. This work utilizes a matrix-based scaling factor to adaptively address image-dependent

variances, in contrast to typical approaches that rely on a single scalar value for scaling. Particle swarm optimization (PSO) is employed to determine appropriate scaling factors [16].

Particle swarm optimization, developed by Kennedy and Eberhart in 1995 [17], is an evolutionary computing method influenced by the social and movement behaviors of biological swarms, including bird flocks, fish schools, and insect colonies. Particle Swarm Optimization (PSO), as a population-based metaheuristic algorithm, has similarities with other metaheuristic optimization methods, such as Genetic algorithms (GAs) or Ant Colony Optimization (ACO). Its strengths, being easy to implement, requiring minimum computation efforts, and being gradient-free, make it extremely beneficial for non-linear and high-dimensional search spaces, particularly [16] [18].

In particle swarm optimization (PSO), each solution is represented as particles, and a group of particles is called a swarm. These particles move through the n-dimensional search space by changing their location and velocity according to individual and social intelligence. Every particle evaluates two crucial performances

- pbest (personal best): the best solution found by the particle so far.
- Global Best (gbest) The best answer found by the whole swarm or in its proximity.

If a particle is in each iteration, its current location is updated based on the interaction of velocity, divergence from pbest, and divergence from gbest. The particle's fitness is determined by problem-specific or, in this case, an objective function that evaluates how imperceptible a watermark can get, depending on its robustness.

Let s represent the swarm size, and for each particle $i(1 \leq i \leq s)$, the subsequent attributes are delineated:

- Current position: $x_i(t)$ in the search space.
- Current velocity: $v_i(t)$.
- Personal best position: $p_i(t)$.
- Global best position: $p_g(t)$ across all particles.

The particle updates are governed by the following Eq. (6) and (7):

$$\mathbf{x_i(t+1) = x_i(t) + v_i(t)} \quad (6)$$

$$\mathbf{v_i(t+1) = \chi[v_i(t) + c_1 r_1\left(p_i - x_i(t)\right) + c_2 r_2(p_g - x_i(t))]} \quad (7)$$

Where:

- $x_i(t+1)$: updated position of a particle i.
- $v_i(t+1)$: updated velocity of a particle i.
- χ: Constriction coefficient to guarantee convergence.
- c_1 and c_2: acceleration coefficients that dictate the impact of individual and collective optimal locations, respectively
- r_1 and r_2: random variables evenly distributed in the interval [0, 1].

The constriction coefficient χ is calculated as follows:

$$\chi = \frac{2\omega}{|2-\phi-\sqrt{\phi^2-4\phi}|} \quad (8)$$

Where $\phi = \phi_1 + \phi_2, \phi_1 = c_1 r_1, \phi_2 = c_2 r_2, and\ \omega \in [0,1]$ is the inertia weight that controls exploration and exploitation trade-offs.

The objective function used in the optimization process is designed to balance imperceptibility and robustness by combining PSNR and NCC. A detailed formulation and justification of this objective function are provided in Section 7.3. The PSO algorithm minimizes the negative of the objective function to simultaneously enhance watermark imperceptibility (increased PSNR) and robustness (higher NCC). The PSO approach determines the optimal scaling factor α through the previously indicated fitness function, therefore reconciling these competing objectives. Refer to Table 1: Detailed Configuration of

PSO settings for Watermark Embedding for a comprehensive list of values for these PSO settings.

7. Watermarking scheme

The watermarking system has three steps: the embedding process, the extraction process, and the scaling factor optimization.

7.1. Embedding process

The block diagram of the suggested design is illustrated in Figure 3, encompassing the stages outlined in the following paragraphs.

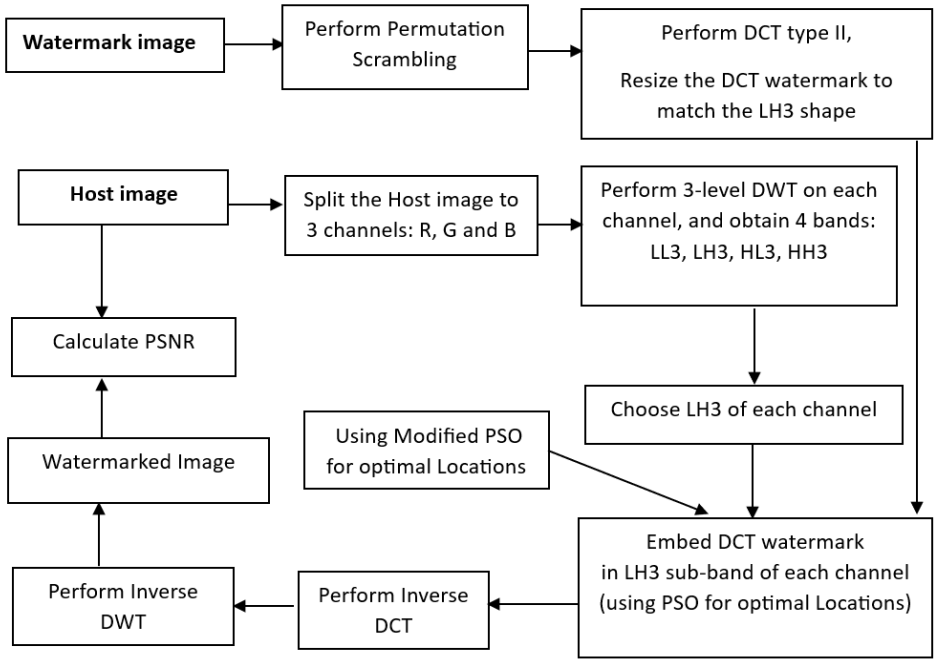

Figure 3: Block Diagram of the Embedding Process

The watermark image is transformed by initially flattening it into a one-dimensional array, permuting the components with permutation indices, and subsequently molding it back into its original two-dimensional form, as shown in Figure 2.

Following this, the 2D DCT Type II is applied to the permuted watermark image. Then, the resultant DCT coefficients are resized to conform to the dimensions of the LH3 sub-band utilizing Eq. (5).

Meanwhile, a three-level discrete Wavelet Transform (DWT) is applied to the host image by using the Daubechies 2 (DB2) family for four sub-bands (LL3, LH3, HL3, and HH3), one for each color channel. DB2 wavelet has compact support and orthonormal properties, which are decent for application in image processing. DWT equations from the DB2 wavelet filter the image in both horizontal and vertical orientations by applying a low-pass filter using Eq. (3) over a high-pass filter using Eq. (4) downsample. These subbands can be described by scaling coefficients ($h[n]$) and wavelet coefficients ($g[n]$ in each filter, which is finally used to transform into these filters. The LL3 sub-band contains low-frequency components, and the other sub-bands contain small image variations. While LL3 retains the majority of visual energy, embedding inside LL3 poses a risk of significant degradation due to its sensitivity to low-frequency perturbations. LH3 was selected as a compromise band because it offers superior imperceptibility compared to LL3 while providing sufficient energy for robust watermarking. LH3 is therefore an optimal sub-band for embedding, as it provides a balance between robustness and perceptual transparency.

The proposed method is a hybrid DWT-DCT watermarking scheme, where the DCT coefficients of the permuted watermark are embedded into the LH3 sub-band of the DWT-transformed cover image. To carry out the embedding, a particle swarm optimization (PSO) technique is employed. The PSO algorithm, inspired by the social behavior of birds, is used to determine suitable embedding locations within the frequency domain. Its main objective is to identify optimal embedding positions that minimize both embedding cost and host image distortion, ensuring the watermark remains imperceptible.
Finally, to obtain the watermarked image, inverse discrete wavelet transform (IDWT) is applied independently to each color channel (R, G, B) after embedding the DCT-permuted watermark into their respective LH3 sub-bands. Each reconstructed channel is then combined to form the final RGB watermarked image. Next, the permuted watermark is inverse-DCT transformed (IDCT) to return it to the spatial domain. Finally, the Peak Signal-to-Noise Ratio (PSNR) is calculated between the original image and the watermarked image to quantify the watermarking quality and distortion, as shown in **Table 7**. A higher PSNR value indicates better image quality and improved watermark concealment.

7.2. Extraction process

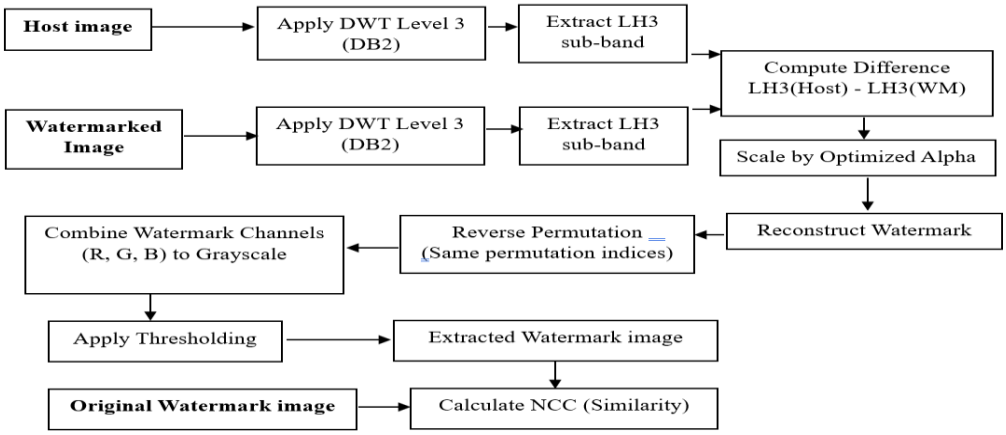

Figure 4: Block diagram of the extraction process.

1. In the first step, the extraction process compares high-frequency detail coefficients of the original and watermarked image. The coefficients are compared, and then the difference is scaled by a factor to get the initial watermark with distortions.
2. After all, the extracted watermark is processed through the Inverse discrete cosine transform (IDCT) so it may be reconstructed from the frequency domain to the spatial domain and made suitable for further analysis.
3. Reverse permutation uses the same permutation key to rearrange the watermark back to its original order and sequence.
4. Combined watermark is thresholded for noise removal to increase the clarity of the watermark, with strong critical top concern.
5. After that, a thresholding operation is applied on both combined watermarks to remove the noise, provided one looks clear, which is the essence of the image.
6. The Correlation between the original and extracted watermark in Normalized Cross-Correlation (NCC) is calculated for measuring the quality of recovery. If NCC is higher, then it shows a more accurate extraction process.

7.3. Optimization of scaling factors using PSO

The proposed method employs particle swarm optimization, illustrated in Figure 5 to determine the best scaling factor (α) for watermark embedding (Section 7.1) and extraction (Section 7.2); the imperceptibility and robustness of the watermarking scheme are significantly

influenced by α. A lower value of alpha α enhances imperceptibility but undermines robustness. A greater alpha α increases resilience but diminishes imperceptibility. Consequently, identifying the best value of alpha α is essential for attaining equilibrium between these conflicting aims.

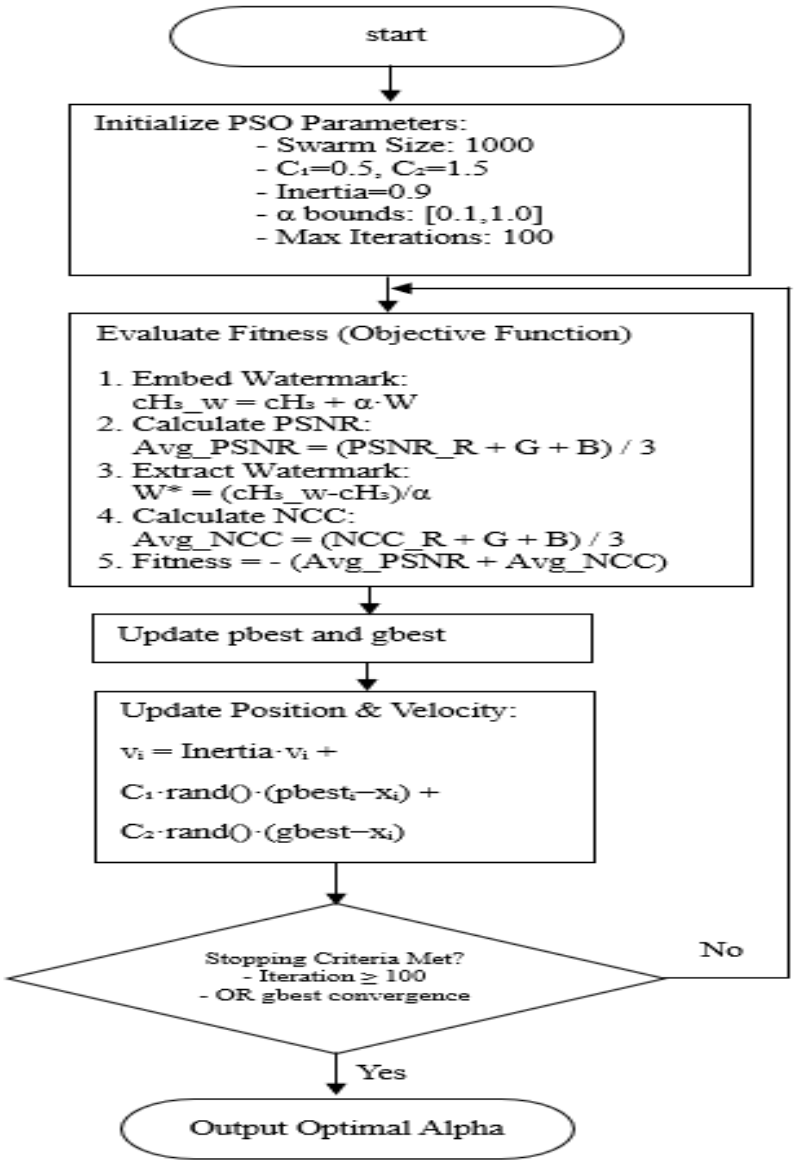

Figure 5. PSO Flowchart of Optimization Process Using Particle Swarm Optimization (PSO) for Alpha Selection in Watermark Embedding

Imperceptibility (I): measured as the correlation between the original image or cover image (C) and the watermarked image (C_w):

$$\boldsymbol{I = correlation(C, C_w)} \quad \textbf{(9)}$$

Robustness (R): measured as the correlation between the original watermark image (W) and the extracted watermark image (W^*):

$$\mathbf{R = correlation(W, W^*)} \quad \textbf{(10)}$$

Where correlation is calculated as:

$$\mathbf{Correlation(X, X^*)} = \frac{\sum_{i=1}^{n}\sum_{j=1}^{n} \mathbf{X(i,j).X^*(i,j)}}{\mathbf{n\ x\ n}} \quad \textbf{(11)}$$

Here, $n\ x\ n$ is the size of the original image.

The fitness function (Objective Function) aims to optimize both imperceptibility (PSNR) and resilience (NCC) by integrating them into a singular scalar objective. By reducing the negative

of this aggregated value, the PSO method aims to identify the best scaling factor α that attains an effective equilibrium between these two opposing objectives, as well as the fitness function Error is characterized as:

$$\mathbf{Error} = -(\mathbf{Avg_{PSNR}} + \mathbf{Avg_{NCC}}) \quad (12)$$

$$\mathbf{Error} = -(\mathbf{Objective\_Value}) \quad (13)$$

Where:

- Avg_PSNR is the mean Peak Signal-to-Noise Ratio across the R, G, and B channels of both the cover image and the watermarked image. This quantifies imperceptibility as per Eq. (14).
- Avg_NCC is the mean Normalized Cross-Correlation between the original watermark and the derived watermark over the R, G, and B channels. This assesses robustness as per Eq. (15).

$$\mathbf{Avg_{PSNR}} = \frac{\mathbf{PSNR_R + PSNR_G + PSNR_B}}{3} \quad (14)$$

$$\mathbf{Avg_{NCC}} = \frac{\mathbf{NCC_R + NCC_G + NCC_B}}{3} \quad (15)$$

Where $PSNR_{channel}$ is the PSNR calculated for each color channel (R, G, B), and $NCC_{Channel}$ is the NCC calculated for each color channel between the original watermark and the extracted watermark.

And the objective value Eq. (16).

$$\mathbf{Objective_{Value}} = \mathbf{Avg_{PSNR}} + \mathbf{Avg_{NCC}} \quad (16)$$

PSO method tunes α 100 times to find out the best α that gives a maximum sum of combined imperceptibility and resilience to make it reproducible, we have defined the random seeds, and the greenest particle swarm optimization configuration is used. This proposed strategy uses PSO at this level for a globally optimal equilibrium between imperceptibility and robustness, in a manner that watermarked images will be imperceptibly perturbed but at the same time be highly resistant to attacks. There must be an optimal α to carry out the embedding/extraction process as shown in trials. In addition, other further regulating factors are depicted in Table 1.

Table 1: Detailed Configuration of PSO Parameters for Watermark Embedding

Parameters	*values*
C1	0.5
C2	1.5
Inertia	0.9
Iteration	100
Number of particles	1000
Bound	[0.1, 1.0]

8. Results and discussions

This study utilizes five distinct color images: 'Lena', 'Cameraman', 'Splash', 'Peppers', and 'Mandrill'. All host images are sized at 512 × 512 pixels. Two distinct grayscale images, 'W1' and 'W2', each measuring 32 × 32, are utilized as watermark images. Fig. 6 displays the host and watermark images. PSNR in Eq. (17) and Normalized Cross Correlation in Eq. (19) are employed to assess the similarity between watermarked images and host images, as well as between extracted and original watermarks, respectively.

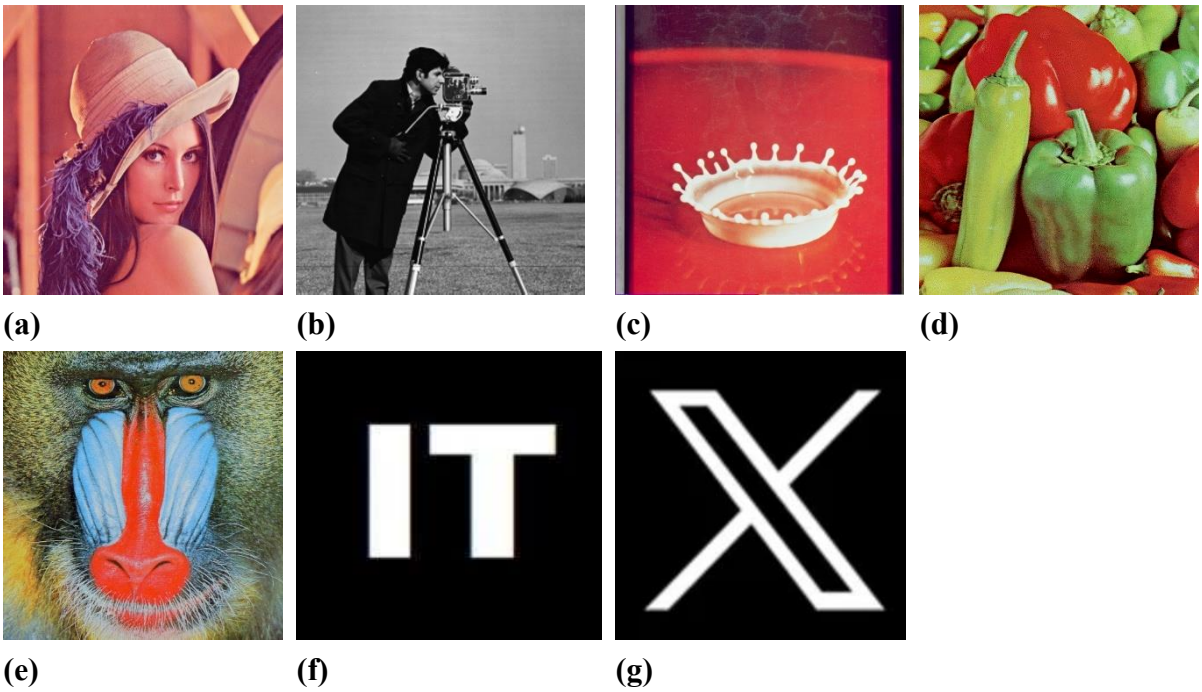

Fig. 6. Host Images and Watermarks: (a) Lena (b) Cameraman (c) Splash (d) Peppers (e) Mandrill (f) W1 (g) W2

Host image (original image) $\boldsymbol{X}$ and watermarked image $\boldsymbol{X^*}$ both have dimensions $\boldsymbol{n} \times \boldsymbol{n}$, where $\boldsymbol{n}$ signifies the pixel of each image. Each can have an image reach a maximal pixel value: $\boldsymbol{X\_max}$ In other words, the Peak Signal-to-Noise Ratio (PSNR) is used to measure how good the watermarked version of the image is compared to the host image:

$$\mathbf{PSNR} = \mathbf{10}.\mathbf{log_{10}}\left(\frac{\mathbf{X_{max}}}{\sqrt{\mathbf{MSE}}}\right) \quad (17)$$

MSE (Mean Squared Error), as defined in Eq. (18), is the average squared deviation between comparable pixel values of the host and watermarked pictures. A greater PSNR value signifies superior quality, whereas an infinite PSNR denotes similar pictures.

$$\mathbf{MSE} = \frac{\mathbf{1}}{\mathbf{n}.\mathbf{m}}\sum_{\mathbf{i=1}}^{\mathbf{n}}\sum_{\mathbf{j=1}}^{\mathbf{m}}(\mathbf{I_o(i,j)} - \mathbf{I_w(i,j)})^{\mathbf{2}} \quad (18)$$

Where:

- n , m are the dimensions of the image.

The Normalized cross-correlation (NCC) quantifies the similarity between the original image X and the watermarked image X^*, while considering variations in their mean pixel values. The NCC is computed by initially ascertaining the average pixel values of both images. The numerator of the NCC equation represents the aggregate of the products of the deviations of pixel values from their respective averages, whilst the denominator normalizes this aggregate by the product of the square roots of the sums of squared deviations for each image. The NCC is characterized as:

$$\mathbf{NCC(X,X^*)} = \frac{\sum_{\mathbf{i=1}}^{\mathbf{n}}\sum_{\mathbf{j=1}}^{\mathbf{n}}(\mathbf{X(i,j)} - \boldsymbol{\mu}_{\mathbf{x}})\,(\mathbf{X^*(i,j)} - \boldsymbol{\mu}_{\mathbf{X^*}})}{\sqrt{\sum_{\mathbf{i=1}}^{\mathbf{n}}\sum_{\mathbf{j=1}}^{\mathbf{n}}(\mathbf{X(i,j)} - \boldsymbol{\mu}_{\mathbf{x}})^{\mathbf{2}}\ \sum_{\mathbf{i=1}}^{\mathbf{n}}\sum_{\mathbf{j=1}}^{\mathbf{n}}(\mathbf{X^*(i,j)} - \boldsymbol{\mu}_{\mathbf{X^*}})^{\mathbf{2}}}} \quad (19)$$

where μ_x and μ_{X^*} Eq. (20) represents the mean pixel values of the host and watermarked images, respectively. The NCC value spans from -1 to 1, with values approaching 1 signifying greater similarity between the images.

$$\boldsymbol{\mu}\mathbf{1} = \frac{\mathbf{1}}{\mathbf{n}.\mathbf{m}}\sum_{\mathbf{i=1}}^{\mathbf{n}}\sum_{\mathbf{j=1}}^{\mathbf{m}}\mathbf{I_1(i,j)}\,,\ \ \boldsymbol{\mu}\mathbf{2} = \frac{\mathbf{1}}{\mathbf{n}.\mathbf{m}}\sum_{\mathbf{i=1}}^{\mathbf{n}}\sum_{\mathbf{j=1}}^{\mathbf{m}}\mathbf{I_2(i,j)} \quad (20)$$

As seen in Figure 8 and Figure 9, the experiment encompasses different steps of images: the host image, two watermark images (W1 and W2), a permuted watermark image, a DCT-

permuted watermark image, and the associated watermarked images. Both watermark images (W1 and W2) were embedded utilizing the identical methodology, although they are processed independently. The permuted watermark is produced using a permutation, but the DCT-permuted watermark is obtained by first performing a permutation followed by the DCT. The ultimate watermarked images are derived by integrating each watermark type into the host image, as elucidated in Section 3.1, enabling a performance comparison. The retrieved watermarks, seen in Figure 7, exhibit an NCC of 1.000 before any attack. Additionally, Fig. 10 illustrates the results of various attacks on the Lena image, which serves as the host, with W1 and W2 representing the watermark images. Moreover, Fig. 11 presents examples of extracted watermark images following several sorts of attacks on the watermarked image.

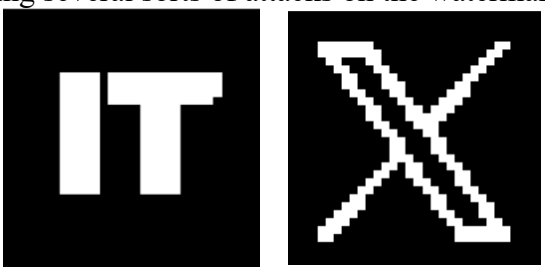

(a) W1 **(b) W2**

Figure 7: Extraction of W1 and W2 Before Attack, Achieving an NCC of 1.000

(a) **(b)** **(c)** **(d)** **(e)**

Figure 8: Embedding Process: (a) Cover image, (b) W1, (c) Permuted W1, (d) DCT on Permuted W1, (e) Watermarked Image

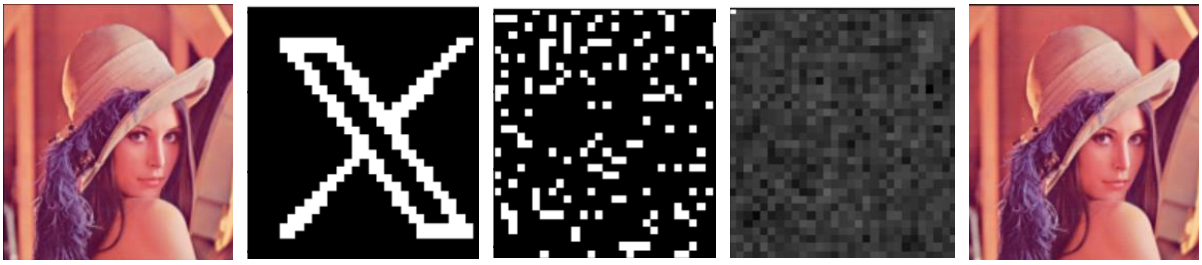

(a) (b) (c) (d) (e)

Figure 9: Embedding Process: (a) Cover image, (b) W2, (c) Permuted W2, (d) DCT on Permuted W2, (e) Watermarked Image

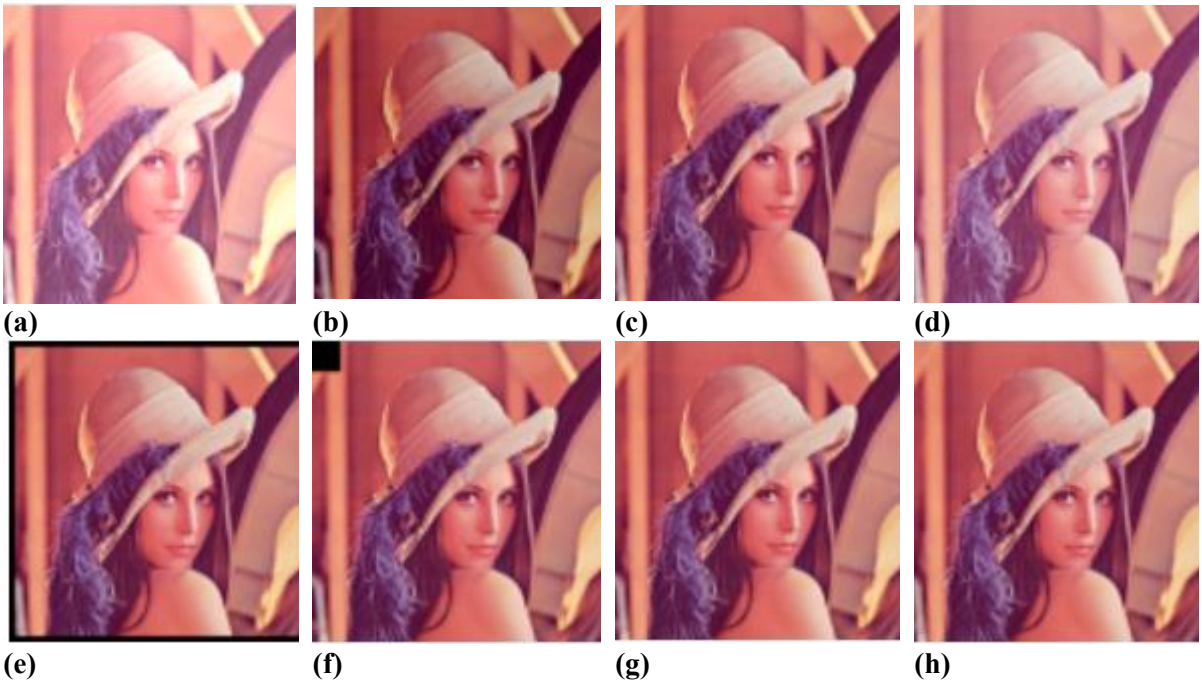

Figure 10: Attacked Watermarked Images: (a) image brightening, (b) darkened image, (c) histogram Equalization, (d) Gamma Corrected Bright, (e) cropped border (20px each side), (f) cropped image (10%), (g) Multiplicative noise (0.03), (h) Gaussian noise (0.1)

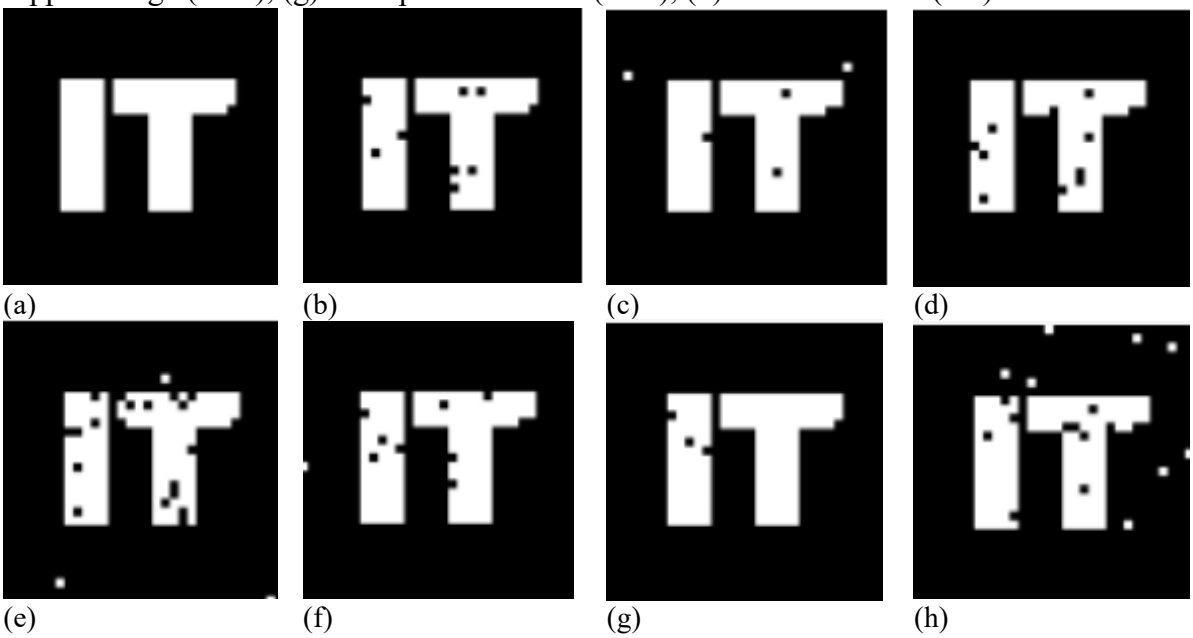

Figure 11: Extracted watermarks W1 after: (a) JPEG, (b) Contrast weaken, (c) Speckle noise (0.04), (d) salt and pepper (0.01), (e) JPG compression (Q=60), (f) Mean filter (3x3), (g) Gaussian-LPF (k=3, sigma=1.0), (h) Cropped image (10%).

Comparative Analysis of PSNR Values and Visual Perception for the Watermarked Image. After embedding the watermark, a comparison of the Peak Signal-to-Noise Ratio (PSNR) values is provided between the suggested watermarking approach and those from three further studies, as shown in **Table 7**. The proposed technique offers a high PSNR that suggests watermarked images have greater visual quality, together with lower distortion. This implies that the suggested approach exhibits better imperceptibility, with embedding watermarks more efficiently than the other kinds of methods, protecting the host image intact.

Table 2 shows various kinds of attacks and the Normalized Cross-Correlation (NCC) between Lena and Cameraman host images using W1 and W2 as watermark images. The results show how the suggested approach is resilient to different conditions.

Table 3 includes Comparisons of attack categories on various cover images, including Splash and Pepper, using the NCC range to establish the robustness of the methodology.

Table 4 shows many attacking types on a Mandrill host image and their NCC values, with the constant efficacy of which the suggested approach shows when carried out on a Mandrill host image.
All these results separately reinforce the robustness of the proposed watermarking scheme against different host images and their attacks.

Table 2.: Types of Attacks on Lena and Cameraman (Cover Images) with W1 and W2 (Watermarks) and Their NCC Values

Attack/image	*Lena*		*Cameraman*	
	W1	W2	W1	W2
	PSNR: 49.0729 dB	PSNR: 49.3103 dB	PSNR: 49.0531 dB	PSNR: 49.3099 dB
No attack	1.0000	1.0000	1.0000	1.0000
JPEG2000 compression (quality 80)	1.0000	1.0000	1.0000	0.9964
JPEG2000 compression (quality 70)	1.0000	1.0000	1.0000	0.9964
JPEG2000 compression (quality 60)	1.0000	1.0000	1.0000	0.9964
Gaussian noise (0.001)	1.0000	1.0000	1.0000	0.9964
Gaussian noise (0.01)	1.0000	1.0000	1.0000	0.9964
Gaussian noise (0.1)	1.0000	1.0000	1.0000	0.9964
Blur (0.3)	1.0000	1.0000	1.0000	0.9964
Contrast adjustment (1.1)	1.0000	0.9927	0.9768	0.9818
Brightness adjustment (0.9)	1.0000	0.9964	0.9768	0.9818
Contrast weakens	0.9735	0.9854	0.8748	0.9223
Image brightening	1.0000	1.0000	0.9801	0.9561
Darkened image	1.0000	1.0000	0.4461	0.4201
Multiplicative noise	1.0000	1.0000	0.9835	0.9781
Speckle noise (0.01)	1.000	1.0000	1.0000	0.9964
Speckle noise (0.04)	0.9801	0.9818	0.9567	0.9567
Sharpening	1.0000	1.0000	1.0000	0.9964

Salt and pepper noise (0.01)	0.8042	0.8378	0.7319	0.7989
Salt and pepper noise (0.001)	0.9702	0.9708	0.9468	0.9598
Compressed image JPEG, 80	0.9701	0.9708	0.9934	0.9927
Compressed image JPEG, 70	0.9635	0.9891	0.9934	0.9818
Compressed image JPEG, 60	0.9237	0.9263	0.9934	0.9745
Histogram Equalization	1.0000	1.0000	1.0000	0.9964
Median filtered image (3x3)	0.9801	0.9818	0.9340	0.8920
Mean filter (3x3)	0.9668	0.9708	0.7857	0.8033
Averaging filter, kernel 3	0.9868	0.9708	0.7381	0.8033
Gaussian low-pass filter, kernel 3	0.9934	0.9891	0.8640	0.8766
Gamma corrected dark (0.9)	0.9934	0.9927	0.9702	0.9671
Gamma corrected bright (1.5)	0.9602	0.9781	0.7818	0.8081
Cropped with borders (10%)	0.5909	0.6225	0.5135	0.5082
Rotation (0.2)	0.7995	0.8115	0.5106	0.5730
Scaling (0.5)	0.9934	0.9891	0.9032	0.8804
Color reduction (50)	1.0000	1.0000	1.0000	1.0000
Cropped image, 10%	0.9370	0.9854	0.8446	0.8688
Cropped image, 25%	0.7915	0.7500	0.5897	0.5656

Table 3: Types of Attacks on Splash and Pepper (Cover Images) with W1 and W2 (Watermarks) and Their NCC Values

Attack/image	*Splash*		*Pepper*	
	W1 PSNR: 49.0729 dB	W2 PSNR: 49.3103 dB	W1 PSNR: 49.0729 dB	W2 PSNR: 49.3103 dB
No attack	1.0000	1.0000	1.0000	1.0000
JPEG2000 compression (quality 80)	1.0000	1.0000	1.0000	1.0000
JPEG2000 compression (quality 70)	1.0000	1.0000	1.0000	1.0000
JPEG2000 compression (quality 60)	1.0000	1.0000	1.0000	1.0000
Gaussian noise (0.001)	1.0000	1.0000	1.0000	1.0000
Gaussian noise (0.01)	1.0000	1.0000	1.0000	1.0000
Gaussian noise (0.1)	1.0000	1.0000	1.0000	1.0000
Blur (0.3)	1.0000	1.0000	1.0000	1.0000
Contrast adjustment (1.1)	0.9967	1.0000	0.9901	0.9927
Brightness adjustment (0.9)	1.0000	1.0000	0.9901	0.9927
Contrast weakens	0.9934	1.0000	0.9399	0.9634
Image brightening	1.0000	0.7781	1.0000	1.0000
Darkened image	1.0000	1.0000	1.0000	1.0000
Multiplicative noise	1.0000	0.9964	0.9705	0.9751
Speckle noise (0.01)	1.0000	1.0000	1.0000	1.0000
Speckle noise (0.04)	0.9934	0.9964	0.9312	0.9388
Sharpening	1.0000	1.0000	1.0000	1.0000
Salt and pepper noise (0.01)	0.7526	0.7764	0.8059	0.8340
Salt and pepper noise (0.001)	0.9802	0.7764	0.9602	0.9671
Histogram equalization	0.9967	0.9964	1.0000	1.0000
Median filtered image (3x3)	0.9967	1.0000	0.8029	0.8115
Mean filter (3x3)	0.9967	1.0000	0.8870	0.9052

Averaging filter, kernel 3	0.9967	1.0000	0.8870	0.9052
Gaussian low-pass filter, kernel 3	0.9967	1.0000	0.9331	0.9486
Gamma corrected dark (0.9)	0.9901	0.9927	1.0000	0.9964
Gamma corrected bright (1.5)	0.9428	0.9262	0.8901	0.8970
Rotation (0.2)	0.8954	0.9320	0.4921	0.5059
Scaling (0.5)	0.9967	1.0000	0.9568	0.9744
Color reduction, 50	0.9967	1.0000	0.9868	0.9964
Cropped image, 10%	0.9835	0.9818	0.8002	0.8452

Table 4: Types of Attacks on Mandrill (Cover Images) with W1 and W2 (Watermarks) and Their NCC Values

Attack/image	*Mandrill*	
	W1	W2
	PSNR: 49.0729 dB	PSNR: 49.3103 dB
No attack	1.0000	1.0000
JPEG2000 compression (quality 80)	1.0000	1.0000
JPEG2000 compression (quality 70)	1.0000	1.0000
JPEG2000 compression (quality 60)	1.0000	1.0000
Gaussian noise (0.001)	1.0000	1.0000
Gaussian noise (0.01)	1.0000	1.0000
Gaussian noise (0.1)	1.0000	1.0000
Blur (0.3)	1.0000	0.9964
Contrast adjustment (1.1)	0.9901	0.9854
Brightness adjustment (0.9)	0.9934	0.9927
Contrast weakens	0.8808	0.8936
Image brightening	0.8883	1.0000
Darkened image	1.0000	1.0000
Multiplicative noise	0.9901	0.9891
Speckle noise (0.01)	1.0000	1.0000
Speckle noise (0.04)	0.9570	0.9639
Sharpening	1.0000	1.0000
Salt and pepper noise (0.01)	0.7595	0.7947
Salt and pepper noise (0.001)	0.9266	0.9524
Compressed image JPEG, 80	0.6682	0.8962
Compressed image JPEG, 70	0.6897	0.8515
Compressed image JPEG, 60	0.6639	0.8428
Histogram equalization	1.0000	1.0000

Gamma corrected dark (0.9)	0.9934	1.0000
Gamma corrected bright (1.5)	0.7116	0.7200
Scaling (0.5)	0.7838	0.7716
Color reduction, 50	1.0000	1.0000
Cropped image, 10%	0.7852	0.9745

Tables 5 and 6 provide a comparative analysis of the robustness of the suggested technique for Normalized Cross-Correlation (NCC) with data from two more research studies. Table 5 contrasts the NCC values for the Lena image, illustrating the superiority of the suggested approach under many situations. Table 6 similarly assesses the resilience of the Mandrill image as the host, demonstrating that the suggested approach surpasses the alternative approaches in almost all circumstances. The results highlight the resilience and security of the proposed method, suggesting its use in actual robust watermarking systems.

Table 5: Performance Comparison of NCC Values for Various Methods Under Different Attacks (Lena Image)

Attacks	*[19]*	*[20]*	*Proposed*
No attack	-	0.98	**1.0000**
Median filter (3x3)	0.9232	0.97	**0.9818**
Mean filter (3x3)	0.9419	-	**0.9708**
Averaging filter 3x3	-	0.94	**0.9708**
JPEG compression (80)	0.9239	-	**0.9708**
JPEG compression (70)	0.9766	1	**0.9891**
Histogram equalization	0.9733	1	**1.0000**
Gaussian noise (0.5)	0.9800	-	**1.0000**
Scaling factor, 0.5	0.8506	0.98	**0.9891**
Scaling factor, 1.5	0.9433	-	**1.0000**
Gaussian filter, 3x3	-	0.98	**0.9891**
Image sharpening	-	1	1.0000
Image cropping 25%	-	0.67	**0.7500**
Gaussian noise (0.001)	-	1	1.0000
Gaussian noise (0.005)	-	0.97	**1.0000**
Gaussian noise (0.01)	-	0.84	**1.0000**

Table 6: Performance Comparison of NCC Values for Various Methods Under Different Attacks (Mandril Image)

Attacks	*[21], single scale*	*[22]*	*Proposed*
No attack	0.9981	0.9940	**1.0000**
JPEG compression (quality 70)	-	0.8470	**0.8515**
Histogram equalization	0.9452	0.8761	**1.0000**
Salt and pepper noise (0.01)	0.8273	0.9761	0.7947
low-pass filter	0.9980	0.9991	0.6949
Multiplicative noise (0.03)	0.8189	0.9554	**0.9891**

Gaussian noise (0.005)	0.9082	-	**1.0000**
Gaussian noise (0.05)	-	0.8466	**1.0000**
Gaussian noise (0.01)	0.8273	0.9653	**1.0000**
Image brightening	0.9779	06010	**1.0000**
Image darkening	0.9777	0.8517	**1.0000**

Table 7: Comparison of PSNR Values and Visual Perception for the Watermarked Image After Embedding the Watermark

Watermarked image	*PSNR*			
	[23]	[24]	[5]	**Proposed**
Image of Lena	44.2229 dB	39.2776 dB	37.23 dB	**49.0729 dB**
Image of Mandrill	44.2292 dB	35.0721 dB	38.12 dB	**49.0729 dB**
Image of pepper	43.7612 dB	34.5422 dB	38.29 dB	**49.0729 dB**
Image of cameraman	-	35.0923 dB	-	**49.0531 dB**
Image of Jet	43.6164 dB	-	-	**49.1646 dB**
Image of Splash	44.1816 dB	-	-	**49.3103 dB**

9. Conclusion

The watermarking method in distinctive portions of the novel suggests resilient and secure image protection that achieves a perfect blend of imperceptibility with robustness. The method combines permutation and discrete cosine transform (DCT), and DWT (hybrid embedding methodology) using particle swarm optimization (PSO), which results in a remarkable increase in security and resistance to various attacks on watermarked images. The experimental results are shown in comparison tables and demonstrate that the proposed scheme outperforms all others in Normalized Cross-Correlation (NCC) and Peak Signal-to-Noise Ratio (PSNR), thus demonstrating the efficiency of watermark integrity preservation and visual distortion reduction. The robustness of the method is additionally supported by strong theoretical justifications, especially after extensive testing on a variety of host images like Lena and Mandrill, indicating that it works for different sorts of images. The best scaling factor, α, which allows an optimal compromise between imperceptibility and robustness, is required so the suggested approach can be applied in practice for secure image watermarking.

References

[1] A. A. M. B. Qazzaz and N. E. Kadhim, "Watermark Based on Singular Value Decomposition," *Baghdad Science Journal*, vol. 20, no. 5, pp. 1797–1807, 2023, doi: 10.21123/bsj.2023.7168.

[2] M. A. Hosen, S. H. Moz, S. S. Kabir, M. N. Adnan, and S. M. Galib, "In-depth exploration of digital image watermarking with discrete cosine transform and discrete wavelet transform," Jan. 01, 2024, *Institute of Advanced Engineering and Science*. doi: 10.11591/ijeecs.v33.i1.pp581-590.

[3] A. Rana, N. Lakshmi, and A. Vaishnav, "Transform domain image watermarking using DCT, DWT and SVD," *International Journal of Innovative Technology and Exploring Engineering*, vol. 8, no. 12, pp. 4323–4331, Oct. 2019, doi: 10.35940/ijitee.L2733.1081219.

[4] N. , R. D. , & D. S. K. Yadav, "Optimization of Watermarking in Image by Using Particle Swarm Optimization Algorithm," *6th International Conference on Signal Processing and Communication (ICSC)*, pp. 85–90, Sep. 2020, doi: 10.1109/ICSC48311.2020.9182716.

[5] T. Zhu, W. Qu, and W. Cao, "An optimized image watermarking algorithm based on SVD and IWT," *Journal of Supercomputing*, vol. 78, no. 1, pp. 222–237, Jan. 2022, doi: 10.1007/s11227-021-03886-2.

[6] F. Yasmeen and M. S. Uddin, "An Efficient Watermarking Approach Based on LL and HH Edges of DWT–SVD," *SN Comput. Sci.*, vol. 2, no. 2, Apr. 2021, doi: 10.1007/s42979-021-00478-y.

[7] I. Iwut, G. Budiman, and L. Novamizanti, "Optimization of discrete cosine transform-based image watermarking by genetics algorithm," *Indonesian Journal of Electrical Engineering and Computer Science*, vol. 4, no. 1, pp. 91–103, Oct. 2016, doi: 10.11591/ijeecs.v4.i1.pp91-103.

[8] T. T. Takore, P. Rajesh Kumar, and G. Lavanya Devi, "A new robust and imperceptible image watermarking scheme based on hybrid transform and PSO," *International Journal of Intelligent Systems and Applications*, vol. 10, no. 11, pp. 50–63, Nov. 2018, doi: 10.5815/ijisa.2018.11.06.

[9] Laxmanika and P. K. Singh, "Robust and imperceptible image watermarking technique based on SVD, DCT, BEMD and PSO in wavelet domain," *Multimed. Tools Appl.*, vol. 81, no. 16, pp. 22001–22026, Jul. 2022, doi: 10.1007/s11042-021-11246-8.

[10] M. Hema and P. S. S, "An Improved Hybrid DCT-DWT Blind Watermarking Technique for Securing Multimedia Images," Feb. 22, 2022. doi: 10.21203/rs.3.rs-1352507/v1.

[11] V. Ch, D. A. Khan, and P. V. S. S. R. Chandramouli, "Digital Watermarking Using Hybrid Grasshopper Optimization Algorithm and Genetic Algorithm (HGOAGA)," *International Journal of Experimental Research and Review*, vol. 42, pp. 278–291, 2024, doi: 10.52756/ijerr.2024.v42.024.

[12] M. Hamidi, M. El Haziti, H. Cherifi, and M. El Hassouni, "A hybrid robust image watermarking method based on dwt-dct and sift for copyright protection," *J. Imaging*, vol. 7, no. 10, Oct. 2021, doi: 10.3390/jimaging7100218.

[13] I. H. Latif, S. H. Abdulredha, and S. K. A. Hassan, "Discrete Wavelet Transform-Based Image Processing: A Review," *Al-Nahrain Journal of Science*, vol. 27, no. 3, pp. 109–125, Sep. 2024, doi: 10.22401/ANJS.27.3.13.

[14] H. K. Khammas and A. K. Türkben, "Adaptive Lossy Color Image Compression System Based on Hybrid Algorithm," *Baghdad Science Journal*, Dec. 2024, doi: 10.21123/bsj.2024.9837.

[15] R. Sripradha and K. Deepa, "Robust and Imperceptible Digital Image Watermarking Based on DWT-DCT-Schur," in *Communications in Computer and Information Science*, Springer Science and Business Media Deutschland GmbH, 2021, pp. 337–351. doi: 10.1007/978-981-16-0425-6_25.

[16] V. Sivavenkateswara Rao, Rajendra S. Shekhawat, and V. K. Srivastava, "A DWT-DCT-SVD Based Digital Image Watermarking Scheme Using Particle Swarm Optimization," *IEEE Students' Conference on Electrical, Electronics and Computer Science*, p. 1, 2012, doi: doi:10.1109/sceecs.2012.6184795.

[17] M. Clerc and J. Kennedy, "The Particle Swarm-Explosion, Stability, and Convergence in a Multidimensional Complex Space," 2002.

[18] P. K. Muhuri, Z. Ashraf, and S. Goel, "A Novel Image Steganographic Method based on Integer Wavelet Transformation and Particle Swarm Optimization," *Applied Soft Computing Journal*, vol. 92, Jul. 2020, doi: 10.1016/j.asoc.2020.106257.

[19] P. Sridhar, "A Robust Digital Image Watermarking in Hybrid Frequency Domain," 2018. [Online]. Available: www.sciencepubco.com/index.php/IJET

[20] Rahim. Esgandari and M. Khalili, "A Robust Image Watermarking Scheme Based on Discrete Wavelet Transforms," Nov. 2015.

[21] N. R. Zhou, A. W. Luo, and W. P. Zou, "Secure and robust watermark scheme based on multiple transforms and particle swarm optimization algorithm," *Multimed. Tools Appl.*, vol. 78, no. 2, pp. 2507–2523, Jan. 2019, doi: 10.1007/s11042-018-6322-9.

[22] N. R. Zhou, W. M. X. Hou, R. H. Wen, and W. P. Zou, "Imperceptible digital watermarking scheme in multiple transform domains," *Multimed. Tools Appl.*, vol. 77, no. 23, pp. 30251–30267, Dec. 2018, doi: 10.1007/s11042-018-6128-9.

[23] G. Pandusarani and A. S. Girsang, "IMPROVED WATERMARKING PERFORMANCE IN COLOR IMAGES THROUGH A HYBRID OF DWT-DCT INTEGRATION FOR COPYRIGHT PROTECTION," 2024, doi: 10.36418/syntax-literate.v9i4.

[24] H. Gao and Q. Chen, "A robust and secure image watermarking scheme using SURF and improved Artificial Bee Colony algorithm in DWT domain," *Optik (Stuttg).*, vol. 242, Sep. 2021, doi: 10.1016/j.ijleo.2021.166954.